





The role of Lagrangian drift in the geometry, kinematics and dynamics of surface waves

Nick Pizzo¹,†, Luc Lenain¹, Olav Rømcke², Simen Å. Ellingsen² and Benjamin K. Smeltzer^{2,3}

(Received 25 August 2022; revised 4 November 2022; accepted 30 November 2022)

The role of the Lagrangian mean flow, or drift, in modulating the geometry, kinematics and dynamics of rotational and irrotational deep-water surface gravity waves is examined. A general theory for permanent progressive waves on an arbitrary vertically sheared steady Lagrangian mean flow is derived in the Lagrangian reference frame and mapped to the Eulerian frame. A Lagrangian viewpoint offers tremendous flexibility due to the particle labelling freedom and allows us to reveal how key physical wave behaviour arises from a kinematic constraint on the vorticity of the fluid, inter alia the nonlinear correction to the phase speed of irrotational finite amplitude waves, the free surface geometry and velocity in the Eulerian frame, and the connection between the Lagrangian drift and the Benjamin–Feir instability. To complement and illustrate our theory, a small laboratory experiment demonstrates how a specially tailored sheared mean flow can almost completely attenuate the Benjamin-Feir instability, in qualitative agreement with the theory. The application of these results to problems in remote sensing and ocean wave modelling is discussed. We provide an answer to a long-standing question: remote sensing techniques based on observing current-induced shifts in the wave dispersion will measure the Lagrangian, not the Eulerian, mean current.

Key words: surface gravity waves, air/sea interactions, ocean processes

† Email address for correspondence: npizzo@ucsd.edu

¹Scripps Institution of Oceanography, University of California San Diego, La Jolla, CA 92037, USA

²Department of Energy Process Engineering, Norwegian University of Science and Technology, N-7491 Trondheim, Norway

³SINTEF Ocean, Marinteknisk senter, N-7052 Trondheim, Norway

1. Introduction

The aim of this paper is to examine the impact of the Lagrangian mean flow, or equivalently the vorticity of the fluid, on the geometry of surface waves, their phase speed, as well as their stability properties. We find that for weakly nonlinear waves on a second-order Lagrangian mean flow, the free surface geometry does not depend on the Lagrangian mean flow to third order in the wave slope. The phase speed is modified by the Lagrangian mean flow at second order, which impacts (and can annihilate) the growth rates of the modulation instability. These results imply that instruments that use the dispersion relationship of waves, e.g. radars or optical imagery systems, measure the Lagrangian mean currents.

Currents modulate the geometry, kinematics and dynamics of deep-water surface gravity waves. The behaviour of linear inviscid waves on a shear flow has typically been examined in the Eulerian reference frame; the literature is large and spans multiple decades, e.g. Peregrine (1976), Jonsson (1990), Shrira (1993), Thomas & Klopman (1997), Ellingsen & Li (2017) and numerous others. However, if the Lagrangian frame is instead used as the point of reference, the explicit role of Lagrangian drift, or equivalently the vorticity of the system, clarifies the origins of several defining characteristics of irrotational and rotational surface gravity waves.

The inverse problem – inferring information about the underlying currents from the wave field – is a central aim of remote sensing instruments. Starting with the pioneering work of Stewart & Joy (1974) and continuing to this day (e.g. Smeltzer et al. 2019), researchers have tried to constrain the underlying structure of currents from measurements of the wave field. However, even in the seminal paper of Stewart & Joy (1974) there is confusion about the impact of the Lagrangian mean flow on the wave phase speed. Specifically, Stewart & Joy (1974) point out that a substitution of the Stokes drift as a current into their theory yields the finite amplitude Stokes correction to the phase speed. However, their theory is Eulerian and hence substituting a Lagrangian mean flow for their mean Eulerian current is inconsistent. Therefore, the correct conclusion was reached via an erroneous argument, resulting in some lingering confusion as to how the Lagrangian mean is connected to the phase speed of water waves as well as the free surface geometry. Here, we clarify these points and show, in particular, that the phase speed is affected by the Lagrangian, not the Eulerian, mean current, thus answering a long-standing question in remote sensing of currents (Chavanne 2018): measured Doppler shifts of surface waves do indeed include the Stokes drift.

A formulation for permanent progressive deep-water waves on a horizontally homogeneous steady shear flow is presented. The governing equations are conservation of mass and conservation of vorticity. The conservation of mass does not specify how particles are to be labelled in a fluid, and this gauge choice (Salmon 2020) offers tremendous freedom in how one approaches problems in this reference frame. At the free surface we require the pressure to vanish while we assume that the waves are in deep-water and hence their induced velocity vanishes at large depths. This leads to a series of coupled equations for the coefficients of the physical locations of particles (a, b) at (x(a, b), y(a, b)), which are much more complicated than their Eulerian counterparts (Clamond 2007) as these series no longer represent analytic functions and hence cannot be related at the surface via the Hilbert transform. We derive the dynamic (pressure) boundary condition in the Lagrangian frame for permanent progressive waves which allows us to relate the Lagrangian mean flow and the phase speed of waves. Additionally, we present new general relationships between the Lagrangian mean flow and the vorticity of the waves.

As an illustration, we consider the response of the surface wave field to a weak, possibly vanishing, Lagrangian mean flow. The finite amplitude correction to the Stokes drift is shown to result in a Doppler-like shift to the frequency of these waves, which explains the curious conclusion of Stewart & Joy (1974). The finite amplitude Stokes correction to phase speed sets the growth rate of the Benjamin–Feir instability (BFI) (Benjamin & Feir 1967; Zakharov 1968) and hence in turn there is a connection between the Lagrangian mean flow (which sets the phase speed) and the strength of this instability, as was originally noted in Abrashkin & Pelinovsky (2017). Here, we explicitly present the growth rate of the most unstable mode and the range of unstable wavenumbers as a function of the Lagrangian mean flow.

To highlight the striking connection between the Lagrangian mean flow and the instability of finite amplitude waves, a laboratory demonstration is presented. We consider two cases, one with approximately no vertical shear (similar to Melville 1982), and another with an imposed shear profile that nearly cancels the Stokes drift of irrotational waves. Radically different long-time behaviour is observed in the two cases. In particular, we find the BFI is largely attenuated due to the presence of the imposed shear, with wave properties closely resembling those of Gerstner more so than Stokes. Note, a full discussion of the laboratory experiments will be presented elsewhere (manuscript in preparation).

2. Governing equations

Consider inviscid deep-water surface gravity waves. The Euler equations in Lagrangian coordinates are (Lamb 1932; Bennett 2006)

$$\mathcal{J}\ddot{x} + p_a y_b - p_b y_a = 0, (2.1)$$

$$\mathcal{J}\ddot{y} + p_b x_a - p_a x_b + \mathcal{J}g = 0, \tag{2.2}$$

where (x, y) are the particle locations with the undisturbed free surface at y = 0, (a, b) are particle labels, p is the kinematic fluid pressure, g is the acceleration due to gravity, and \mathcal{J} is defined as

$$\mathcal{J} = \frac{\partial(x, y)}{\partial(a, b)} \equiv x_a y_b - x_b y_a = \left[\frac{\rho(a, b)}{\rho(x, y)}\right]^{-1},\tag{2.3}$$

for ρ the fluid density and subscripts denoting partial derivatives. The continuity equation may be written

$$u_{x} + v_{y} = \frac{\partial(\dot{x}, y)}{\partial(x, y)} - \frac{\partial(\dot{y}, x)}{\partial(x, y)} = \left(\frac{\partial(\dot{x}, y)}{\partial(a, b)} - \frac{\partial(\dot{y}, x)}{\partial(a, b)}\right) \frac{\partial(a, b)}{\partial(x, y)} = \frac{1}{\mathcal{J}} \frac{d\mathcal{J}}{dt} = 0, \quad (2.4)$$

where $u = \dot{x}$, $v = \dot{y}$ with dots representing differentiation with respect to time. This implies

$$\frac{\mathrm{d}\mathcal{J}}{\mathrm{d}t} = 0. \tag{2.5}$$

In order for the mapping to be invertible we also require that $\mathcal J$ does not change sign. The vorticity is defined as

$$\Gamma = v_x - u_y = \frac{\partial(v, y)}{\partial(x, y)} + \frac{\partial(u, x)}{\partial(x, y)} = \frac{1}{\mathcal{J}} (\dot{x}_a x_b - \dot{x}_b x_a + \dot{y}_a y_b - \dot{y}_b y_a). \tag{2.6}$$

Equations (2.1) and (2.2) imply that vorticity is conserved, that is $\dot{\Gamma} = 0$. For irrotational flows $\Gamma = 0$. Furthermore, through this discussion we assume $\Gamma \to 0$ as $b \to -\infty$.

The pressure p must vanish at the free surface, which we choose to occur at b = 0 so that p = 0 at b = 0. Finally, we take the bottom to be the limit as $b \to -\infty$, so that $\dot{y} \to 0$ at $b \to -\infty$.

2.1. Series expansions

We consider permanent progressive monochromatic waves progressing with velocity c, so that we assume the map between (x, y) and (a, b) takes the form

$$x = a + U(b)t + \sum_{n=1}^{\infty} x_n(b)\sin\theta_n; \quad y = b + y_0(b) + \sum_{n=1}^{\infty} y_n(b)\cos\theta_n, \quad (2.7a,b)$$

where $\theta_n = nk(a - (c - U(b))t)$, k is the wavenumber and U is the Lagrangian mean flow. We are considering the intrinsic frequency here, as this eliminates secular terms (Buldakov, Taylor & Taylor 2006; Clamond 2007). There is some question as to the convergence of these Lagrangian expansions, which have been formally studied for Gerstner waves (Henry 2008; Constantin 2011). This is discussed in Clamond (2007), where it is shown numerically that there is series convergence even for the highest wave, although the convergence rates are slow. A full discussion of this point is outside of the scope of this manuscript, but here we assume that the expansions given by (2.7a,b) converge. Note, Clamond (2007) assumed that k = k(b) while here we take k as a constant. This changes the values of wave amplitude that give particular values of ak, but all physical quantities remain the same.

The mean surface level, $y_0(0) \equiv \langle y \rangle|_{b=0}$ (here $\langle \dots \rangle = (2\pi/k)^{-1} \int_0^{2\pi/k} (\dots) da$ is phase averaging), is found by inserting (2.7*a*,*b*) into (2.3) and phase averaging to find

$$y_0(b) = -\frac{1}{2} \sum knx_n y_n + \int_{-\infty}^b (\langle \mathcal{J} \rangle - 1) \, \mathrm{d}\beta + y_0^0, \tag{2.8}$$

where y_0^0 is a constant of integration that is determined by the proper choice of the Bernoulli head, ensuring that $\langle yx_a|_{b=0}\rangle=0$. Note, it is understood here and henceforth that an integration variable β replaces b in the integrands, and \sum implies summing n from 1 to ∞ .

The Lagrangian drift arises as a kinematic constraint that requires the vorticity to be time independent, so that from the mean component of the vorticity we find

$$U = \frac{\frac{c}{2} \sum n^2 k^2 (x_n^2 + y_n^2) - \gamma}{1 + \frac{1}{2} \sum n^2 k^2 (x_n^2 + y_n^2)},$$
(2.9)

where $\gamma \equiv \langle \int_{-\infty}^{b} \Gamma \mathcal{J} \, \mathrm{d}\beta \rangle$. This equation implies that if the vertical behaviour is simple in (x_n, y_n) , e.g. of exponential decay form, it will not be simple in U, and vice versa.

From (2.9) we also see that the vorticity and Lagrangian mean flow are intimately related. If we prescribe the vorticity, this then constrains the form of the drift, and vice versa. This will be made clearer in the asymptotic example considered below.

2.2. Free surface pressure condition

Next, we can find other relationships between y_0 , U and c by solving for the pressure. That is, multiplying (2.1) by x_b and (2.2) by y_b , we find

$$p_b + gy_b + \ddot{y}y_b + \ddot{x}x_b = 0. (2.10)$$

Next, by differentiating the series expansions for (x, y) we find $\ddot{y} = -(c - U)\dot{y}_a$, and $\ddot{x} = -(c - U)\dot{x}_a$ so that

$$p_b + gy_b - (c - U)(\dot{y}_a y_b + \dot{x}_a x_b) = 0.$$
 (2.11)

We can rewrite the expression in the final parentheses using the definition of the vorticity, (2.6), to find

$$p_b + gy_b - (c - U)(\Gamma \mathcal{J} + \dot{x}_b x_a + \dot{y}_b y_a) = 0.$$
 (2.12)

We can relate space and time derivatives via $x_a = 1 + ((U - \dot{x})/(c - U))$ and $y_a = -\dot{y}/(c - U)$, so that (2.12) may be written as

$$\left[p + gy + \frac{1}{2}(\dot{x} - c)^2 + \frac{1}{2}\dot{y}^2\right]_b - (c - U)\mathcal{J}\Gamma = 0$$
 (2.13)

$$\implies p + gy + \frac{(\dot{x} - c)^2 + \dot{y}^2}{2} = \int_{-\infty}^{b} (c - U) \Gamma \mathcal{J} \, \mathrm{d}\beta + f(a, t), \tag{2.14}$$

where f(a, t) is a constant of integration which must be $c^2/2$ so that $\langle p(b=0)\rangle = 0$. When $\Gamma = 0$ we return a recognizable form of Bernoulli's equation for irrotational permanent progressive waves.

The dynamic boundary condition requires $\langle p \rangle = 0$ at b = 0, so that we can find an expression for the phase velocity in terms of y_0 and U at the surface (note the constant of integration for y_0 must be correct to employ this – e.g. for Gerstner waves y_0^0 is not zero and is given explicitly in the next section), which yields

$$c = \frac{2gy_0 - U\gamma + 2\int_{-\infty}^0 U\langle \Gamma \mathcal{J}\rangle \,\mathrm{d}\beta}{U + \gamma} \bigg|_{b=0}, \qquad (2.15)$$

where we have used the fact that $\langle \dot{x}^2+\dot{y}^2\rangle=U^2+(c-U)^2\sum n^2k^2(x_n^2+y_n^2)/2=c(\gamma+U)-U\gamma$, which is found by solving for $\sum k^2n^2(x_n^2+y_n^2)$ in (2.9). Equation (2.15) reduces in limiting scenarios. First, when $\Gamma=0$, $c=2gy_0/U|_{b=0}$, while for U=0 we have $c=2gy_0/\gamma|_{b=0}$.

Notice in (2.15) that c is determined by the Lagrangian, not Eulerian, current. Even with zero Eulerian current, c obtains a Doppler-like shift due to Stokes drift. We can then answer the question of Chavanne (2018): the observed Doppler shift of waves do indeed include the Stokes drift as well as the Eulerian current.

In the classical approach to examining Stokes waves in an Eulerian framework, the condition that p=0 at the free surface, together with the analyticity of the velocity potential and stream function, is enough to reduce the problem to a boundary value system which may be solved algebraically (Schwartz 1974; Balk 1996). In the Lagrangian frame it is clear that the velocity potential and stream function do not satisfy the Cauchy–Riemann equations and hence are not analytic. In general, the series expansions for z=x+iy depend on both s=a+ib and $\bar{s}=a-ib$. A simple example is given by Gerstner's wave, which takes the form $kz=ks+i\epsilon$ exp($ik\bar{s}-ikct$) for ϵ a wave slope and c a phase velocity

(Lamb 1932, § 251). We see immediately that $z_{\bar{s}} \neq 0$ and hence z is not analytic. A more general approach is then needed to examine solutions to this system of equations. This will be pursued elsewhere and instead for the rest of the present study we illustrate the physical implications of the Lagrangian drift by considering asymptotic solutions in limiting cases.

3. Weakly nonlinear waves on a weak shear flow

As our starting point we take Gerstner's (Lamb 1932, § 251) remarkable, exact surface wave solution

$$kx = ka - \epsilon \sin(k(a - ct))e^{kb}; \quad ky = \frac{1}{2}\epsilon^2 + kb + \epsilon \cos(k(a - ct))e^{kb}, \quad (3.1a,b)$$

where ϵ is the wave slope. These waves have no mean Lagrangian transport – their particle trajectories are circles. Since U(b)=0, (2.15) implies $c=\sqrt{g/k}$, independent of ϵ . As discussed in Clamond (2007), the mean water level is $k^{-1}\epsilon^2/2$; although not usually written explicitly, this term is crucial to properly compute c. Note, Gerstner waves are finite amplitude exact solutions which possess interesting stability properties of their own (Leblanc 2004; Ionescu-Kruse 2018).

The determinant of the Jacobian of the mapping from physical space to label space is $\mathcal{J} = 1 - \epsilon^2 e^{2kb}$ while the vorticity may be found through the relation $\Gamma \mathcal{J} = 2ck\epsilon^2 e^{2kb}$.

To transform these Lagrangian solutions to the Eulerian frame we must find a = a(x). This inversion is not possible in closed form, as it essentially reduces to solving Kepler's equation and so we must invert this relationship iteratively at each order of ϵ .

Defining η as $\eta = y(a(x), b = 0, t) = y(x, t)$, then to $O(\epsilon^3)$, where $\epsilon \ll 1$, we find

$$ka = kx + \epsilon \sin \theta_0 + \frac{\epsilon^2}{2} \sin 2\theta_0 - \frac{\epsilon^3}{8} (\sin \theta_0 - 3\sin 3\theta_0), \qquad (3.2)$$

at b = 0 so that

$$k\eta = \left(\epsilon - \frac{3\epsilon^3}{8}\right)\cos\theta_0 + \frac{\epsilon^2}{2}\cos 2\theta_0 + \frac{3\epsilon^3}{8}\cos 3\theta_0 + \dots, \tag{3.3}$$

where $\theta_0 = k(x - c_0 t)$ and $c_0 = \sqrt{g/k}$. Note, there is a second-order correction to the mean surface level in the Lagrangian frame, but there is no correction to $O(\epsilon^3)$ in the Eulerian frame (Longuet-Higgins 1986).

We can also find the horizontal and vertical Eulerian velocities (u, v) to $O(\epsilon^3)$. This involves finding a = a(x, y) and b = b(x, y) to third order, which gives

$$ka(x,y) = kx + \left(\epsilon + \frac{\epsilon^3}{2}(1 - e^{2ky})\right)\sin\theta_0 e^{ky},\tag{3.4}$$

$$kb(x, y) = ky - \left(\epsilon + \frac{\epsilon^3}{2}(-1 + 3e^{2ky})\right)\cos\theta_0 e^{ky} + \epsilon^2\left(-\frac{1}{2} + e^{2ky}\right).$$
 (3.5)

Inserting these into (3.1*a*,*b*), the Eulerian velocity fields $(u, v) = (\dot{x}, \dot{y})$ are given by

$$u(x, y, t) = c_0 \left(\epsilon + \frac{\epsilon^3}{2} \left(-1 + 3e^{2ky} \right) \right) \cos \theta_0 e^{ky} - c\epsilon^2 e^{2ky}; \tag{3.6}$$

$$v(x, y, t) = c_0 \left(\epsilon - \frac{\epsilon^3}{2} \left(1 - e^{2ky} \right) \right) \sin \theta_0 e^{ky}, \tag{3.7}$$

so that we see that Gerstner waves require there to be a non-zero horizontal Eulerian mean flow at second order that is equal and opposite to the Stokes drift.

3.1. Third-order weakly rotational and irrotational waves

Next we find the third-order expansions for Stokes waves by expanding the Gerstner waves solutions to include $O(\epsilon^2)$ Lagrangian mean flows, $\epsilon^2 U(b)$ (see also the related discussions in Abrashkin & Pelinovsky 2017, 2018). Going through the algebra, we find

$$kx = ka + kU(b)t - \left(\epsilon e^{kb} + \frac{\epsilon^3}{k}F'(b)\right)\sin\theta_L; \quad ky = kb + \frac{1}{2}\epsilon^2 + \left(\epsilon e^b + \epsilon^3 F(b)\right)\cos\theta_L,$$
(3.8a,b)

where $\theta_L = k(a - (c - \epsilon^2 U)t)$ and $F \equiv (2k/c)e^{-kb} \int_{-\infty}^b e^{2k\beta} U(\beta) \, \mathrm{d}\beta$. Note, the phase now has dependence on b and c is unknown at this stage.

The mean water level y_0 is $O(\epsilon^2)$ in the Lagrangian reference frame, compared with $O(\epsilon^3)$ in the Eulerian frame (Longuet-Higgins 1986).

Insertion into (2.3) and (2.6) gives Jacobian $\mathcal{J} = 1 - \epsilon^2 e^{2kb}$, and vorticity

$$\Gamma = \epsilon^2 (2kce^{2kb} - U'(b)). \tag{3.9}$$

When $U = ce^{2kb}$, the flow is thus irrotational and we return the well-known expansions for Stokes waves to third order in ϵ .

Equation (3.9) is of central importance – it relates the vorticity of the system to gradients of the Lagrangian mean flow. At this order, the right-hand side of (3.9) is the curl operator, so we return a main result from generalized Lagrangian mean theory (Bühler 2014), namely that the vorticity of the system is given by the difference of the curl of the pseudomomentum and the Lagrangian mean flow. A similar equation arises when one allows for finite bandwidth effects and offers a clear motivation for the long wave response, or Bretherton flow, of a wave packet (Salmon 2020; Pizzo & Salmon 2021).

Additionally, the phase velocity c is found to be

$$c = c_0 \left(1 + \epsilon^2 F(0) \right) = c_0 \left(1 + \epsilon^2 \left(\frac{2k}{c_0} \int_{-\infty}^0 e^{2k\beta} U(\beta) \, \mathrm{d}\beta \right) \right). \tag{3.10}$$

When U=0, we return the expansions for the Gerstner wave while for an irrotational wave, $U=c_0e^{2kb}$ and we return the phase velocity with the Stokes correction, i.e. $\frac{1}{2}\epsilon^2$. Note, unlike Stewart & Joy (1974), we have used a consistent argument to return this result.

Inversion methods for inferring the underlying currents from the wave field rely on measuring deviations of the wave phase velocity from that in quiescent waters. The phase velocity deviation in (3.10) implies that such inversion methods are sensitive to the Lagrangian mean flow. A comprehensive analysis would involve considering a broadband wave spectrum with contributions to the Stokes drift from many wavenumbers, which is outside the scope of the present work.

As we did for the Gerstner wave in (3.3), we can map (3.8a,b), under the constraint that the flow is irrotational, to the Eulerian frame, finding

$$k\eta = \left(\epsilon + \frac{\epsilon^3}{8}\right)\cos\theta + \frac{\epsilon^2}{2}\cos 2\theta + \frac{3\epsilon^3}{8}\cos 3\theta + \dots$$
 (3.11)

where $\theta = k(x - ct)$ and $c = c_0(1 + \frac{1}{2}\epsilon^2)$ follows from (3.10).

When comparing (3.11) and (3.3), we see immediately that the second harmonic of η is the same for Gerstner and Stokes waves, and hence is not related to the

Lagrangian mean flow. If we define a new small parameter $\mu = \epsilon - (\epsilon^3/2)$ then $k\eta = (\mu - (3\mu^3/8))\cos\theta + (\mu^2/2)\cos2\theta + (3\mu^3/8)\cos3\theta$, which implies that Stokes waves and Gerstner waves have identical free surface geometries to third order (Clamond 2007).

Additionally, we can find the velocity in the Eulerian frame. Again, we need to write down the depth-dependent mappings:

$$ka(x,y) = kx - c_0 k \epsilon^2 t e^{2ky} + \left(\epsilon + \frac{\epsilon^3}{2} \left(-1 + 4e^{2ky}\right)\right) \sin\theta e^{ky} + 2\epsilon^3 c_0 kt \cos\theta e^{3ky},$$
(3.12)

$$kb(x,y) = ky + \epsilon^2 \left(-\frac{1}{2} + e^{2ky} \right) - \left(\epsilon + \frac{\epsilon^3}{2} \left(-1 + 4e^{2ky} \right) \right) \cos \theta e^{ky}. \tag{3.13}$$

Substituting these relationships into the velocity field for this case of irrotational flow, we find

$$u = \epsilon c \cos \theta e^{ky}; \quad v = \epsilon c \sin \theta e^{ky},$$
 (3.14*a,b*)

which agrees with the classical result for third-order Stokes waves.

Although not considered here, one may also examine mixed Eulerian–Lagrangian maps in the spirit of Virasoro (1981). This may have applications to the interpretation of current measurements from uncrewed mobile platforms like the Liquid Robotics Wave Glider (Grare *et al.* 2021).

3.2. Modulation instability

The form of the phase velocity is enough to provide a heuristic derivation of the nonlinear Schrödinger equation (NLSE) on a weak Lagrangian shear flow (Abrashkin & Pelinovsky 2017), following the classical geometrical optics approach (Benjamin & Feir 1967; Yuen & Lake 1982; Abrashkin & Pelinovsky 2018). Whereas previous, Eulerian derivations of the NLSE in the presence of shear have favoured the special case of constant vorticity which permits potential theory (Baumstein 1998; Thomas, Kharif & Manna 2012); the Lagrangian framework handles arbitrary U(b) more readily.

Here, we take $\epsilon = \epsilon_0 A$ for some complex valued dimensionless amplitude A of O(1), and we drop the subscript on ϵ for clarity of presentation. We regard the reference system where the constant of integration for U in (3.9) is zero, and define

$$\mathcal{V} \equiv 2\frac{k}{c}\epsilon^2 \int_{-\infty}^0 e^{2k\beta} U(\beta) \,\mathrm{d}\beta,\tag{3.15}$$

which implies the dispersion relationship is given by $\omega = \omega_0(1 + \mathcal{V})$ with $\omega_0 = k_0c_0 = \sqrt{gk_0}$ with k_0 the wavenumber of the unmodulated regular wave.

Following Abrashkin & Pelinovsky (2018), we take a geometrical optics approach and let $\omega = \omega_0 + i\epsilon \partial_t$ and $k = k_0 - i\epsilon \partial_x$, where we have expanded about a carrier wave with frequency ω_0 and wavenumber k_0 . Multiplying the dispersion relationship by A, we find that to $O(\epsilon^3)$

$$iA_{\tau} - \frac{1}{9}A_{\gamma\gamma} - 2AV = 0,$$
 (3.16)

where $\tau = \epsilon^2 \omega_0 t$ and $\chi = \epsilon k_0 (x - c_{g0} t)$ where the group velocity is $c_{g0} = \frac{1}{2} c_0$.

A solution to this NLSE, (3.16), is $A = a_0 \exp(-2i\mathcal{V}\tau)$, and we define k_0K and $\omega_0\Omega$ as the wavenumber and frequency of a perturbation to this solution, respectively.

Taking a perturbation of this solution of the form $A = (a_0 + \delta_+ \exp(i(\Omega \tau + K\chi)) + \delta_- \exp(i(\Omega \tau - K\chi))) \exp(-2iV\tau)$, we find that to lowest order in (δ_+, δ_-) the system obeys

$$\begin{pmatrix} 2\mathcal{V} - (K^2/8) - \Omega & 2\mathcal{V} \\ 2\mathcal{V} & 2\mathcal{V} - (K^2/8) + \Omega \end{pmatrix} \begin{pmatrix} \delta_+ \\ \delta_- \end{pmatrix} = \begin{pmatrix} 0 \\ 0 \end{pmatrix}. \tag{3.17}$$

Non-trivial solutions exist when the determinant of the matrix is zero, which implies $\Omega^2 = \frac{1}{9}((K^2/8) - 4V)K^2$.

The system is unstable when V > 0 and

$$0 < K < 4\sqrt{2V},\tag{3.18}$$

while the most unstable wavenumber occurs when $K = 4\sqrt{V}$ with growth rate

$$|\Omega_{max}| = 2\mathcal{V}.\tag{3.19}$$

The relations (3.18) and (3.19), although implicit in Abrashkin & Pelinovsky (2018), were not presented there. We see that the growth rate of the instability may be strongly modified (i.e. it is zero for Gerstner waves) and the range of wavenumbers that are unstable can vary considerably as a function of the drift.

We now discuss a laboratory demonstration of this deep result.

4. Laboratory demonstration of the impact of the Lagrangian mean flow on the Benjamin-Feir instability

The laboratory demonstration discussed below was conducted in the recirculating water channel at Norwegian University of Science and Technology. See Jooss et al. (2021) for further details. The test section is 11.2 m long, 1.8 m wide and is outfitted with a plunger wave maker at the outlet, generating waves propagating upstream on the flow. At the inlet the incoming flow of depth 0.5 m is controlled by an active grid which allows us to tailor the vertical shear. The active grid consists of horizontal and vertical bars spaced by 10 cm with square wings attached, each wing measuring 10 cm along the diagonal. Each bar is controlled by a stepper motor. The five submerged horizontal grid bars were actuated in a flapping motion relative to the position of least flow blockage. We use the flapping to design two flow profiles. For an approximately depth-uniform mean flow, all bars were flapped through an angle of $\pm 45^{\circ}$. A second profile with near-surface vertical shear approximately cancelling the Stokes drift profile was created by keeping the shallowest bar fixed in a position of least blockage while the deeper bars were flapped through an angle of $\pm 60^{\circ}$. The vertical grid bars were always fixed in the position of least blockage. In the centre of the channel eight wave gauges, at locations {1.703, 1.914, 3.719, 3.924, 5.722, 5.929, 7.719, 7.928} metres from the wave maker measured the free surface displacement. Laser Doppler velocimetry (60 mm FiberFlow probe, Dantec Dynamics) was used to measure the near-surface current profiles.

Figure 1 illustrates how the Lagrangian mean flow can alter the BFI growth rates. In particular, when the induced flow has negligible shear, as plotted in figure 1(a), we see the strong groupiness in the wave field, signifying the flux of energy from the finite amplitude carrier waves to the sidebands, which is clear from the spectral plot shown in figure 1(c). The waves have slope 0.17 (–) and wavenumber 6.0 (rad m⁻¹). Strikingly, when an Eulerian mean shear current is generated that approximately cancels the Stokes drift (such that the Lagrangian drift $U \approx 0$), the BFI is strongly suppressed. This is evident by the time

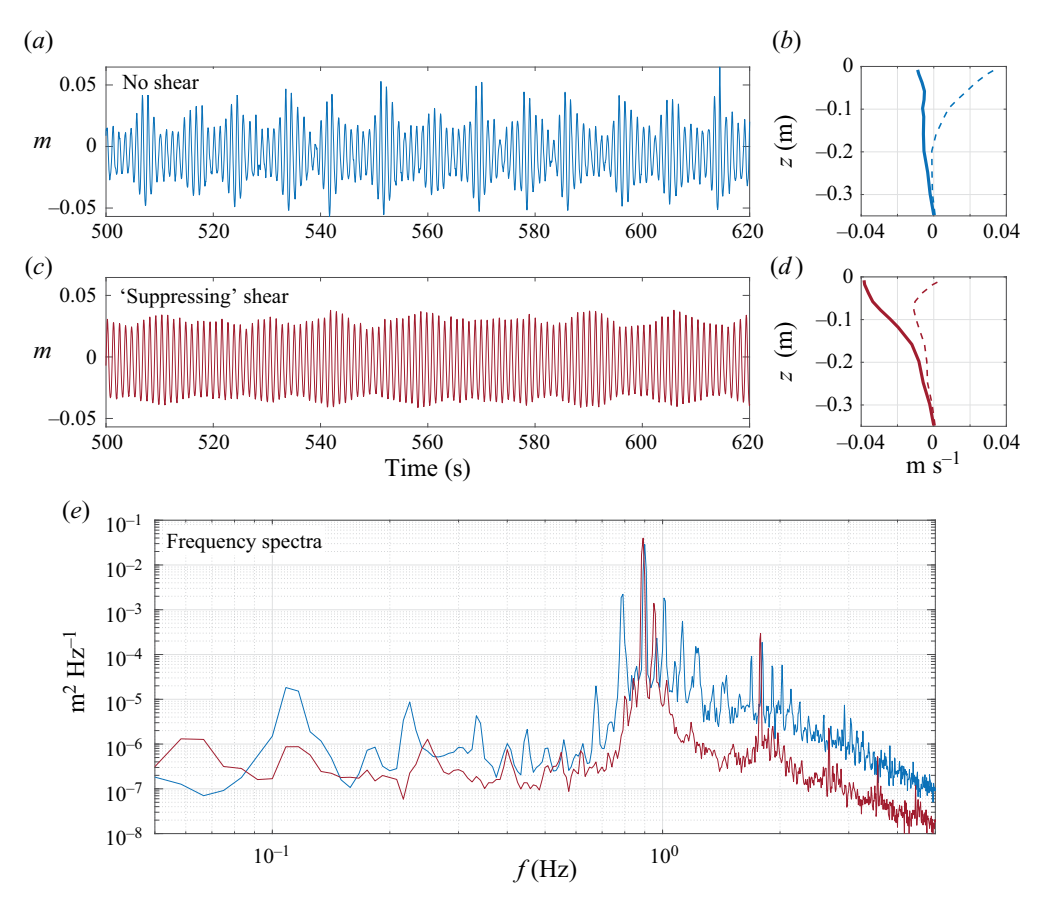


Figure 1. The evolution of finite amplitude surface gravity waves in a wave channel with two imposed shear currents – one that is approximately uniform (a,b) and one whose shear acts to approximately cancel the Stokes drift so that the Lagrangian current $U \approx 0$ (c,d). Steepness and wavenumbers are (a) 0.176 and 6.01 (rad m⁻¹) and (c) 0.174 and 6.06 (rad m⁻¹). Eulerian (Lagrangian) currents are shown with solid (dashed) lines in (b,d) and wave spectra in (e).

series, which shows only weak modulations of the wave amplitude. Correspondingly, we find a far weaker sideband and low-frequency response. The sideband growth is strongly asymmetric, which is not accounted for in the theory. However, the higher frequency sideband is much closer to the carrier wave frequency than in the case of minimal shear, in agreement with (3.18). Note, the waves in figure 1(b) more closely resemble those of Gerstner than those of Stokes. This discussion is meant to serve as a demonstration of the ideas presented in this manuscript, particularly in § 3.2. The BFI weakening from constant mean shear was observed by (Steer *et al.* (2020), see also Simmen & Saffman 1985; Baumstein 1998; Thomas *et al.* 2012); a tailored profile based on the Lagrangian theory enabled this arguably even more striking demonstration. A detailed quantitative analysis, beyond the scope of this manuscript, is currently in preparation.

5. Conclusions

In this paper we have presented a novel formulation for permanent progressive waves on a horizontally uniform time-independent Lagrangian mean. We related fundamental

properties of the waves, *viz*. their vorticity and phase velocity, with the Lagrangian mean flow. We then presented the explicit connection between the Lagrangian mean flow and wave geometry, kinematics and dynamics for the scenario when the Lagrangian mean flow was weak. This included explicit expressions for the dependence of the Benjamin–Feir instability growth rate (Abrashkin & Pelinovsky 2017, 2018), as well as the range of unstable perturbation wavenumbers and frequencies, on the Lagrangian mean flow. To illustrate these points, we presented results from a recent laboratory demonstration that highlight the striking dependence of finite amplitude wave behaviour on the underlying shear flow.

Our theoretical results imply that the nonlinear source term in the wave action evolution equation (Hasselmann 1973; Phillips 1985) should have growth rates that depend on the shear in the underlying flow. In particular, (3.19) shows how the growth rate depends on both the wave slope and the underlying Lagrangian mean flow. If there are external currents, then this can potentially modify the instability growth rates and hence the wave action flux (Longuet-Higgins 1976). As the upper ocean is sheared, a better understanding of the implications of this work for weak wave turbulence are of particular interest and of significant potential impact to the wave modelling community.

Finally, our results can be used to infer information about sub-surface currents based on observations of the surface wave field. We emphasize that it is the Lagrangian, not the Eulerian, current which can be measured remotely from wave dispersion alone. Specifically, the explicit mappings between Lagrangian and Eulerian reference frames for the Stokes and Gerstner waves highlight that the Lagrangian mean does not modulate free surface geometry to third order. Instead the higher order corrections arise due to the nonlinear mapping between the frames. However, the Lagrangian mean flow does show up as a Doppler-like shift to the wave frequency. A comprehensive discussion of a set of laboratory experiments on wave geometry, kinematics and dynamics for waves on a shear flow is in preparation.

Acknowledgements. N.P. thanks R. Salmon for many useful discussions on these topics, which directly motivated the present investigation.

Funding. N.P. and L.L. were partially supported by NSF grant OCE-2219752 and NASA grant 80NSSC19K1688. S.Å.E. was supported by Research Council of Norway grant 325114.

Declaration of interests. The authors report no conflict of interest.

Author ORCIDs.

- Nick Pizzo https://orcid.org/0000-0001-9570-4200;
- Luc Lenain https://orcid.org/0000-0001-9808-1563;
- Olav Rømcke https://orcid.org/0000-0003-0440-7388;
- © Simen Å. Ellingsen https://orcid.org/0000-0002-0294-0405;
- Benjamin K. Smeltzer https://orcid.org/0000-0002-4977-7692.

REFERENCES

ABRASHKIN, A. & PELINOVSKY, E. 2017 Lagrange form of the nonlinear Schrödinger equation for low-vorticity waves in deep water. *Nonlinear Process. Geophys.* 24 (2), 255–264.

ABRASHKIN, A.A. & PELINOVSKY, E.N. 2018 On the relation between Stokes drift and the Gerstner wave. *Phys.-Usp.* **61** (3), 307–312.

BALK, A.M. 1996 A Lagrangian for water waves. Phys. Fluids 8 (2), 416-420.

BAUMSTEIN, A.I. 1998 Modulation of gravity waves with shear in water. *Stud. Appl. Maths* **100** (4), 365–390. BENJAMIN, T.B. & FEIR, J.E. 1967 The disintegration of wave trains on deep water Part 1. Theory. *J. Fluid Mech.* **27** (03), 417–430.

N. Pizzo and others

- BENNETT, A. 2006 Lagrangian Fluid Dynamics. Cambridge University Press.
- BÜHLER, O. 2014 Waves and Mean Flows. Cambridge University Press.
- BULDAKOV, E.V., TAYLOR, P.H. & TAYLOR, R.E. 2006 New asymptotic description of nonlinear water waves in Lagrangian coordinates. *J. Fluid Mech.* 562, 431–444.
- CHAVANNE, C. 2018 Do high-frequency radars measure the wave-induced Stokes drift? *J. Atmos. Ocean. Technol.* **35** (5), 1023–1031.
- CLAMOND, D. 2007 On the Lagrangian description of steady surface gravity waves. J. Fluid Mech. 589, 433–454.
- CONSTANTIN, A. 2011 Nonlinear Water Waves with Applications to Wave-Current Interactions and Tsunamis. SIAM.
- ELLINGSEN, S.Å. & LI, Y. 2017 Approximate dispersion relations for waves on arbitrary shear flows. J. Geophys. Res. 122, 9889–9905.
- GRARE, L., STATOM, N.M., PIZZO, N. & LENAIN, L. 2021 Instrumented wave gliders for air-sea interaction and upper ocean research. *Front. Mar. Sci.* doi:10.3389/fmars.2021.664728.
- HASSELMANN, K. 1973 Measurements of wind wave growth and swell decay during the Joint North Sea Wave Project (JONSWAP). *Dtsch. Hydrogr. Z.* **8**, 95.
- HENRY, D. 2008 On Gerstner's water wave. J. Nonlinear Math. Phys. 15 (sup2), 87–95.
- IONESCU-KRUSE, D. 2018 On the short-wavelength stabilities of some geophysical flows. *Phil. Trans. R. Soc. Lond.* A 376 (2111), 20170090.
- JONSSON, I.G. 1990 Wave-current interactions. The Sea (ed. B. LeMehaute & D.M. Hanes), vol. 9, pp. 65–120.
 JOOSS, Y., LI, L., BRACCHI, T. & HEARST, R.J. 2021 Spatial development of a turbulent boundary layer subjected to freestream turbulence. J. Fluid Mech. 911, A4.
- LAMB, H. 1932 Hydrodynamics, 6th edn. Cambridge University Press.
- LEBLANC, S. 2004 Local stability of Gerstner's waves. J. Fluid Mech. 506, 245–254.
- LONGUET-HIGGINS, M.S. 1976 On the nonlinear transfer of energy in the peak of a gravity-wave spectrum: a simplified model. *Proc. R. Soc. Lond.* A **347** (1650), 311–328.
- LONGUET-HIGGINS, M.S. 1986 Eulerian and Lagrangian aspects of surface waves. *J. Fluid Mech.* 173, 683–707.
- MELVILLE, W.K. 1982 The instability and breaking of deep-water waves. J. Fluid Mech. 115, 165–185.
- PEREGRINE, D.H. 1976 Interaction of water waves and currents. Adv. Appl. Mech. 16, 9–117.
- PHILLIPS, O.M. 1985 Spectral and statistical properties of the equilibrium range in wind-generated gravity waves. *J. Fluid Mech.* **156** (1), 505–531.
- PIZZO, N. & SALMON, R. 2021 Particle description of the interaction between wave packets and point vortices. J. Fluid Mech. 925, A32.
- SALMON, R. 2020 More lectures on geophysical fluid dynamics. http://pordlabs.ucsd.edu/rsalmon/More. Lectures.pdf.
- SCHWARTZ, L.W. 1974 Computer extension and analytic continuation of Stokes expansion for gravity waves. J. Fluid Mech. 62 (3), 553–578.
- SHRIRA, V.I. 1993 Surface waves on shear currents: solution of the boundary-value problem. *J. Fluid Mech.* **252**, 565–584.
- SIMMEN, J.A. & SAFFMAN, P.G. 1985 Steady deep-water waves on a linear shear current. *Stud. Appl. Maths* **73** (1), 35–57.
- SMELTZER, B.K., ÆSØY, E., ÅDNØY, A. & ELLINGSEN, S.Å. 2019 An improved method for determining near-surface currents from wave dispersion measurements. *J. Geophys. Res.* **124**, 8832–8851.
- STEER, J.N., BORTHWICK, A.G.L., STAGONAS, D., BULDAKOV, E. & VAN DEN BREMER, T.S. 2020 Experimental study of dispersion and modulational instability of surface gravity waves on constant vorticity currents. *J. Fluid Mech.* **884**, A40.
- STEWART, R.H. & JOY, J.W. 1974 HF radio measurements of surface currents. *Deep-Sea Res.* 21 (12), 1039–1049.
- THOMAS, G.P. & KLOPMAN, G. 1997 Wave-current interactions in the near shore region. *Intl Ser. Adv. Fluid Mech.* 10, 255–319.
- THOMAS, R., KHARIF, C. & MANNA, M. 2012 A nonlinear Schrödinger equation for water waves on finite depth with constant vorticity. *Phys. Fluids* **24** (12), 127102.
- VIRASORO, M.A. 1981 Variational principle for two-dimensional incompressible hydrodynamics and quasigeostrophic flows. *Phys. Rev. Lett.* 47 (17), 1181.
- YUEN, H.C. & LAKE, B.M. 1982 Nonlinear dynamics of deep-water gravity waves. *Adv. Appl. Mech.* 22 (67), 229.
- ZAKHAROV, V.E. 1968 Stability of periodic waves of finite amplitude on the surface of a deep fluid. *J. Appl. Mech. Tech. Phys.* 9 (2), 190–194.